Supplemental Information:

Additional Methods

HPLC confirmation of dye-polymer conjugate: Reverse-phase HPLC analysis was performed using a 1260 Infinity Quaternary LC System (Agilent Technologies, Santa Clara, CA) using a 50 × 2.0 µm Proto 200 C18, 5 µm column (Higgins Analytical, Mountain View, CA) at room temperature with a 50 µL injection. The ratio of HPLC grade acetonitrile to HPLC grade deionized water (both with 0.1% (v/v) trifluoro acetic acid) was increased from 5% to 95% over 25 min, followed by a 5 min washout phase and a methanol needle wash between sample injections. AF-647 was detected by absorbance at 650 nm.

Confirmation of device size stability: 10 dp devices were fabricated as previously described, and imaged using light microscopy. Devices were then exposed to SGF for 30 min, imaged, and then exposed to SIF adjusted to pH 5 with HCL for 4 hr and imaged a third time. Quantification of device sizes after each exposure was performed using ImageJ.

Additional Results:

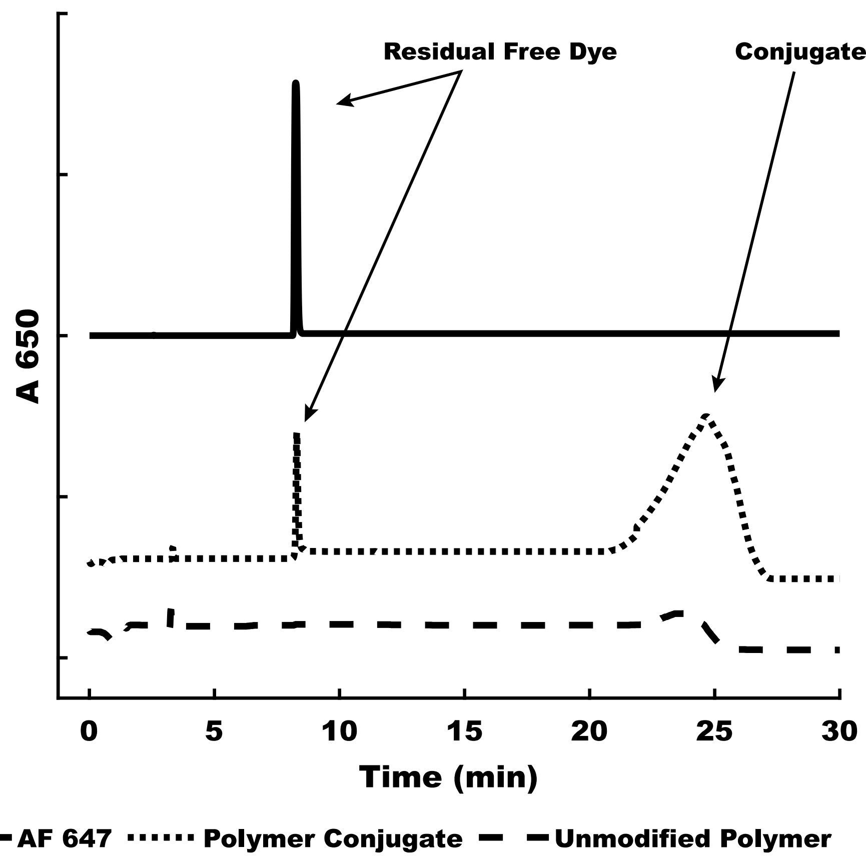

Supplementary Figure 1: HPLC validation of polymer-dye conjugate product. Dye, polymer conjugate, and unmodified polymer samples were prepared fresh in deionized water, at 100 µg/mL for the free dye and 10 mg/mL for the polymer samples. Free dye was observed to elute at 8.2 min, while the dye conjugate was observed to elute at 24.7 min. Free dye represents less than 3% of total signal in labeled polymer sample. Conjugation efficacy was determined via absorbance at 650 nm of a 1 mg/mL solution of the dye-polymer product, demonstrating the addition of approximately 3 µg of dye per mg of polymer, or the conversion of approximately 37% of the initial dye

A.

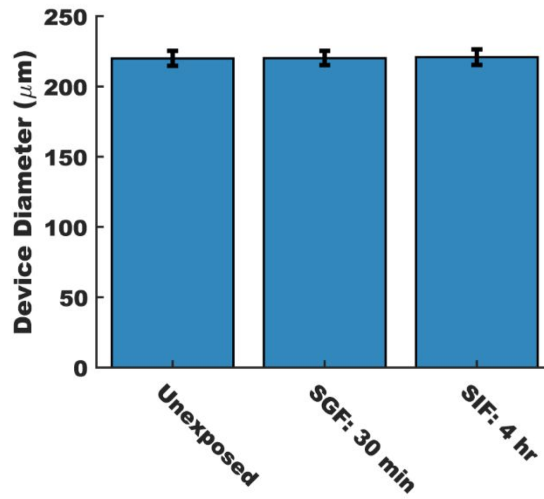

B.

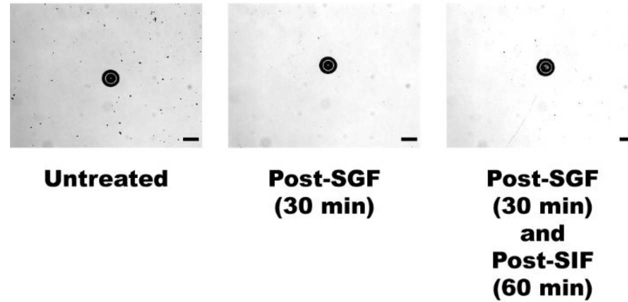

Supplementary Figure 2: Validation of device size stability. (**A**) Repeated measures of same device population pre-exposure, post SGF exposure, and post SGF & SIF (adjusted to pH 5) exposure. Data representative of mean ± 1 SD, of n=37 devices. No differences were detected between groups at α=0.05, using a one-way ANOVA followed by a Tukey-Kramer correction for multiple comparisons. (**B**) Same representative device after each exposure, affixed to a silicon wafer. Scalebar represents 200 μm.

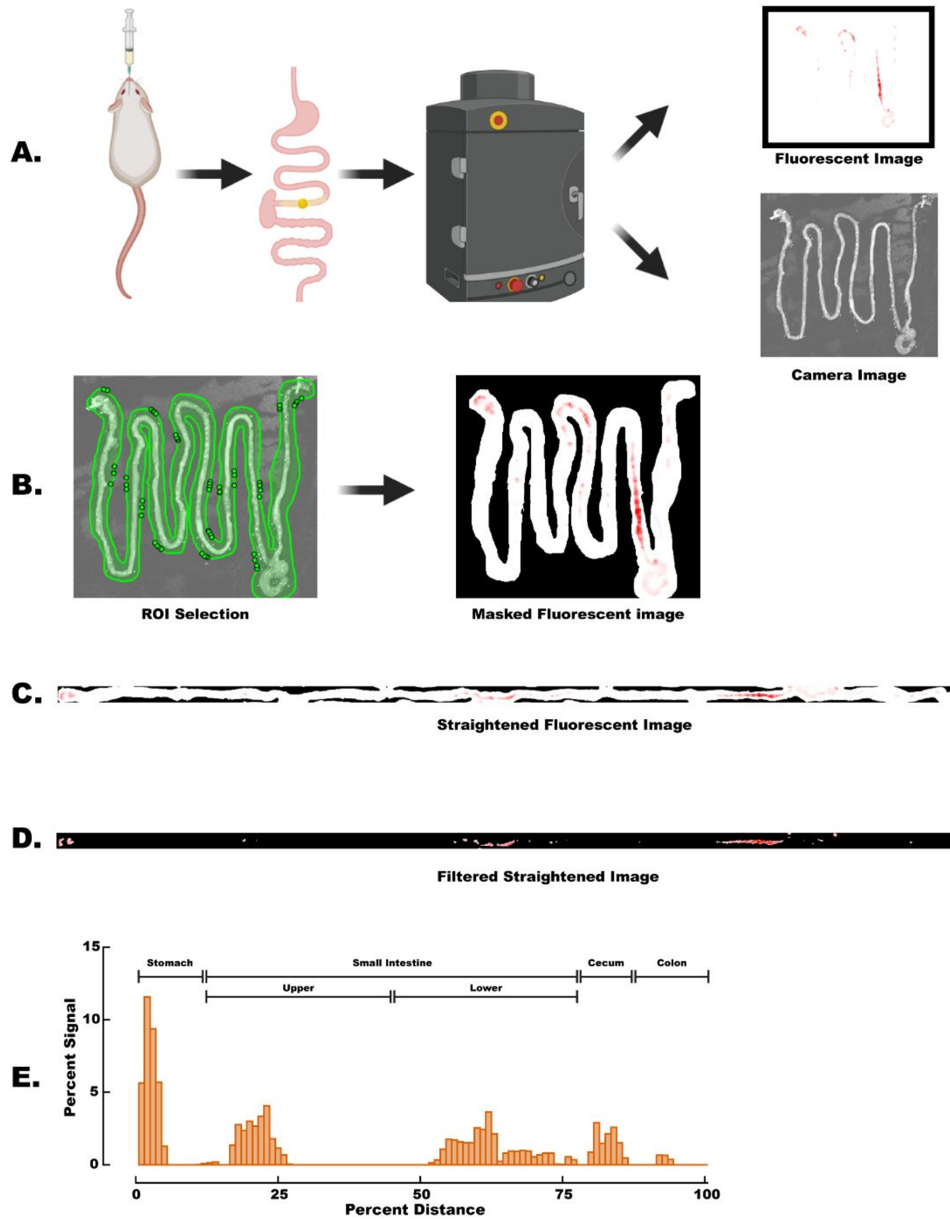

Supplementary Figure 3: Outline of image analysis pipeline for continuous device tracking. **(A)** After dosing with microdevices via oral-gavage, mice are sacrificed at the specified time points (30 min, 60 min, 4 hr). Extracted GI tracts were imaged using a Xenogen Spectrum imaging system, using the standard AF 647 filter set, adjusting the f-stop of the CCD to 1 to increase sensitivity. Imaging each sample produces two distinct images: a digital photograph of the tissue, and a monochromatic trace of the fluorescent signal. **(B)** Using MATLAB scripting, a region of interest (ROI) is traced onto the photograph (by hand), and then applied to the fluorescent image, producing the masked image shown. **(C)** Applying an integrated ImageJ instance within the MATLAB script, the ROI from the masked fluorescent image is selected and straightened as shown, to produce an image of a constant width that captures the entirety of the GI tract. **(D)** The straightened image is imported back into the MATLAB instance, and filtered to remove any pixels not containing red signal using an orthogonal YCbCr color space mask. The RGB image is further processed (not shown) to a mono-chromatic format, leaving only the red channel. **(E)** The resulting matrix of pixel values is summed column-wise to produce a one-dimensional vector of signal information. This data is normalized by the total signal present in the given animal, and plotted as normalized percent signal vs. percent distance along the GI tract. Further, to mitigate some of the inherent volatility in the signal and preserve the inherent patterns in the data, it is compressed in a lossless manner, such that each datapoint represents the sum of signal present in the preceding 1% of the GI tract. On average, the stomach represents the first 15% of the signal, the small intestine the next 60% (split evenly between the upper and lower small intestine), the cecum the next 10%, and the colon the final 15%.

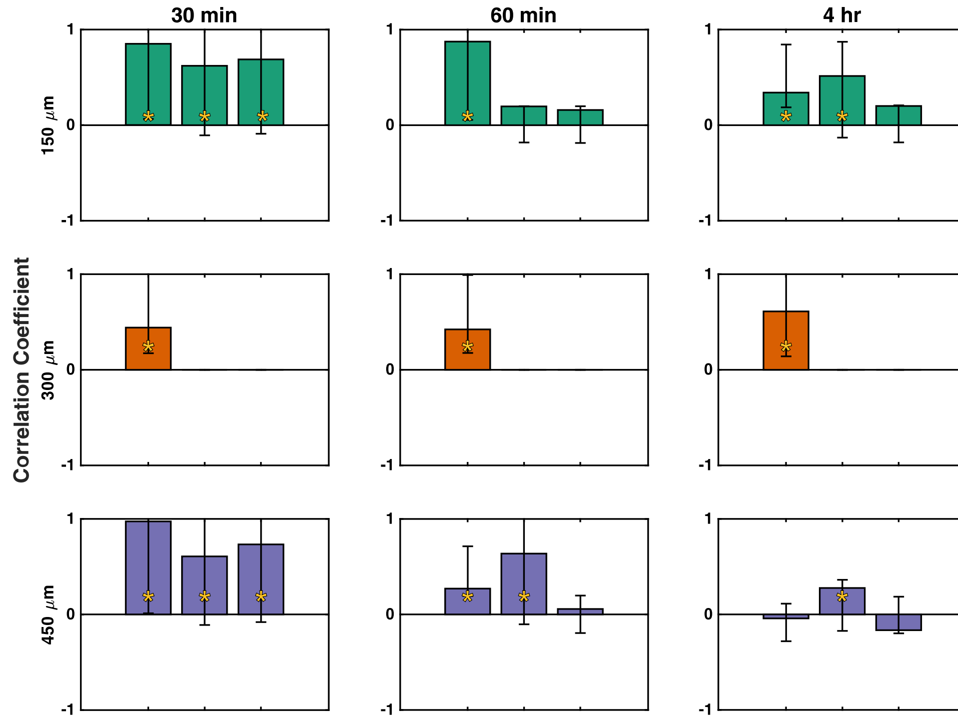

Supplementary Figure 4: Cross-correlation coefficients from pair wise intragroup comparisons of signal vs distance data. Each bar represents one pairwise comparison between two distinct signals, error bars represent the bounds of the 95% confidence interval of the correlation coefficient. Bars marked with * successfully reject the null-hypothesis of no correlation at $\alpha = 0.05$. Unmarked groups fail to reject the null-hypothesis of no correlation between signals. To limit the family wise error rate, p-values were adjusted using a Bonferroni correction for multiple comparisons.

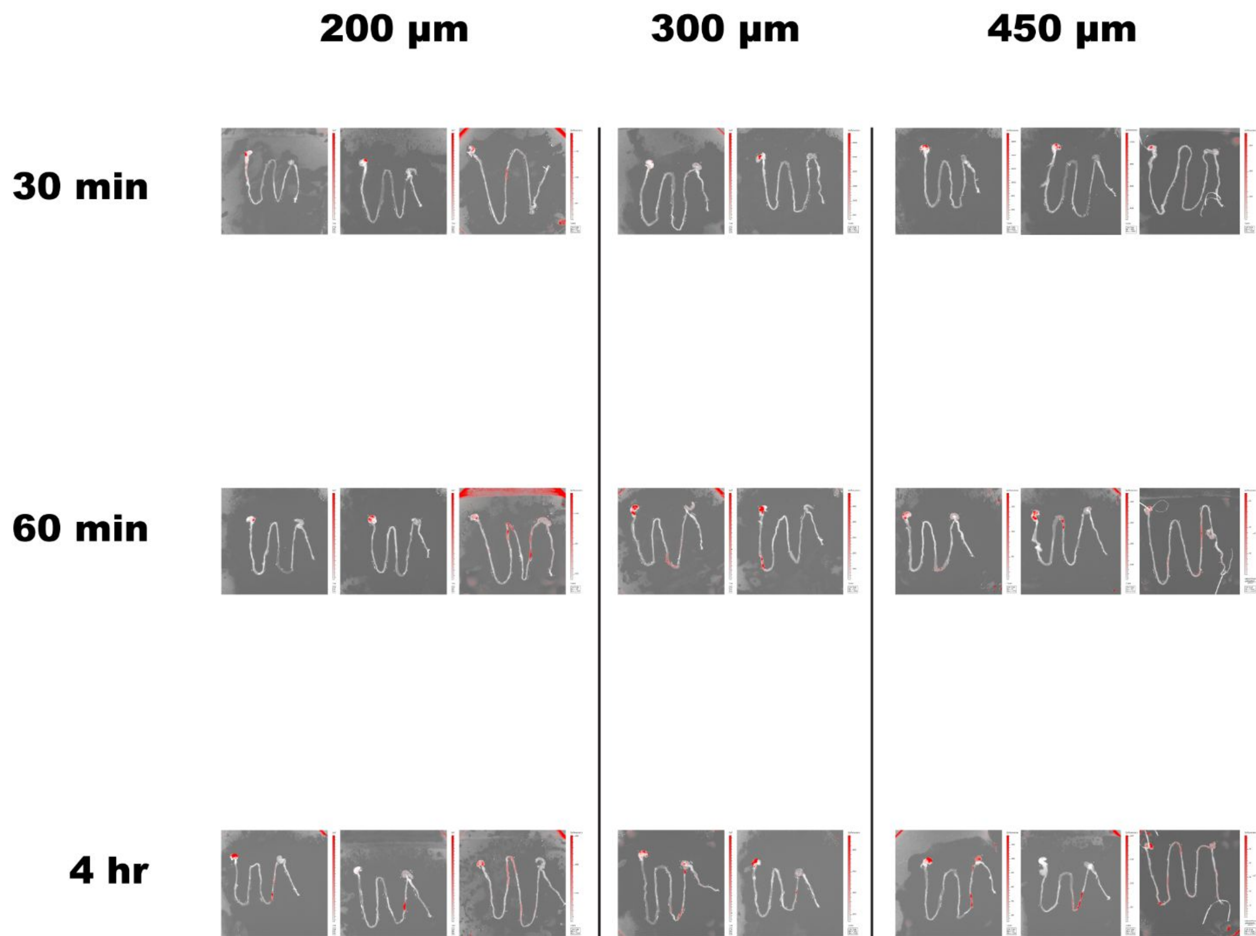

Supplementary Figure 5: Overlayed fluorescent images from all mice used for statistical purposes in this study. Red signal represents fluorescent intensity (measured in photon count) as indicated by the color-bar scale accompanying each image.